Nine Non-symmetric Pyrazine-Pyridine Imide-Based Complexes: Reversible Redox and Isolation of $[M^{II/III}(pypzca)_2]^{0/+}$ when M = Co, Fe

Matthew G. Cowan and Sally Brooker*

Department of Chemistry and the MacDiarmid Institute for Advanced Materials and Nanotechnology, University of Otago, PO Box 56, Dunedin 9054, New Zealand. Fax: +64-3-479 7906; Tel: +64-3-479 7912; E-mail: sbrooker@chemistry.otago.ac.nz

Electronic Supporting Information

Discussion of Unsuccessful Synthetic Routes

$[Mn^{II}(pypzca)_2]$

Reacting $Mn^{II}(ClO_4)_2 \cdot 6H_2O$ with Hpypzca and triethylamine in acetone under a nitrogen atmosphere produced a lightly coloured solid. The mass spectrum showed a small signal corresponding to $[Mn(pypzca)_2Na]^+$, however there were also many other signals corresponding to other manganese and ligand containing fragments. Despite several attempts and washing the product with multiple solvents (including dichloromethane, methanol, acetone and water) in no case did elemental analysis support the formation of a $pypzca^-$ complex. Electrochemical studies of the crude solids did not show any promising processes. Hence a different reaction protocol was tried. Marcos et al. had produced crystals of $[Mn^{II}(bpca)_2]$ by mixing $Mn^{II}(NO_3)_2 \cdot 4H_2O$ and Hbpca in a mixture of acetone and water, using sodium hydroxide to control the pH, and leaving it to slowly evaporate in air.[25] In the analogous reaction with Hpypzca a red/brown solution was obtained. A very small amount of brown precipitate too fine to filter was produced, and a dark coloured tacky residue resulted from slow evaporation of the filtrate.

Our attention then turned to the use of manganese(II) chloride in these reactions with Hpypzca and triethylamine, and this led to the formation of $[Mn^{II}(pypzca)Cl_2]HNEt_3$ (see later). An attempt to convert this complex into $[Mn^{II}(pypzca)_2]$ was made. It was reacted with two equivalents of silver tetrafluoroborate in methanol and the solid AgCl was removed by filtration. The filtrate was added to a solution of Hpypzca and triethylamine in acetone resulting in a small amount of extremely fine, light brown precipitate, which darkened upon drying. The mass spectrum of the solid contained several unassigned species, including a small peak for the expected $[Mn^{II}(pypzca)_2]Na^+$ fragment, indicating that $[Mn^{II}(pypzca)_2]$ does form to some extent. However it is not the only product and we are unable to cleanly produce or isolate it.

$[Fe^{III}(pypzca)_2]X$

Using the colour of the solution as an indicator, it was clear that unlike the cobalt(II) case, spontaneous oxidation of iron(II) to iron(III) was not occurring in the acetone/water reaction solution. The material obtained from these reactions was, according to electrochemistry and UV-Vis spectra, a mixture of $[Fe^{III}(pypzca)_2]BF_4$ and $[Fe^{II}(pypzca)_2]$. In an attempt to complete the oxidation, hydrogen peroxide was added to the reaction solution. However, whilst this resulted in a temporary colour change to pale brown, over time the solution returned to the darker colour. Attempts to use iron(III) reagents including $FeCl_3 \cdot 6H_2O$ and $Fe(NO_3)_3 \cdot 9H_2O$, with Hpypzca and triethylamine, initially resulted in light brown solutions, but the resulting dark solids gave low percentages of carbon, hydrogen and nitrogen that more likely correspond to an iron oxide or hydroxide. To try and avoid this occurring, the use of base was avoided by attempting a transmetallation of $[Zn^{II}(pypzca)_2]$ with iron(III) nitrate in a refluxing mixture of dichloromethane and methanol. The brown solid obtained from diethyl ether diffusion into the reaction solution showed no signal for a $[Fe(pypza)_2]^+$ fragment in the mass spectrum (there was insufficient solid for elemental analysis). Kooijman et. al. have previously reported the preparation of

the analogue $[Fe^{III}(bpca)_2]ClO_4$,[27] so their method was tried next. The amide analogue of Hpypzca, prepared as previously reported,[15] was combined with one equivalent of triethylamine and half an equivalent of $Fe^{II}(BF_4)_2 \cdot 6H_2O$ or $Fe^{II}(ClO_4)_2 \cdot 6H_2O$ in methanol or acetonitrile, respectively. The resulting dark solution did not lighten in colour and a mass spectrum of the amorphous solid obtained was not cleanly either the amide or imide complex of iron(II) or of iron(III).

$[Mn^{III}(pypzca)_2]X$

The manganese(III) complex, $[Mn^{III}(pypzca)_2]Y$ (Y = mono anion), was not successfully synthesised. An attempt to produce the desired complex from the reaction of $Mn^{III}(OAc)_3.2H_2O$, Hpypzca and triethylamine in a mixture of methanol and acetone gave a brown solution. Diethyl ether vapour diffusion into this solution resulted in a brown solid which had a low C, H and N composition inconsistent with that expected for a complex of $pypzca^-$. Given that manganese(III) is a Jahn-Teller active ion, it is possible that binding two $(pypzca)^-$ ligands may be unfavourable, however, against this is the fact that the analogous copper(II) complex has been made (although it appears more labile than other $[M^{II}(pypzca)_2]$ complexes, losing one ligand in the mass spectrometer).

The difficulties encountered in the preparation of these complexes are attributed to a lack of redox stability in the N_6 coordination environment provided by Hpypzca.

Infrared Data

Figure S1. A comparison of the carbonyl stretching bands in $[Co^{II}(pypzca)_2]$ (black) and $[Co^{III}(pypzca)_2]BF_4$ (red).

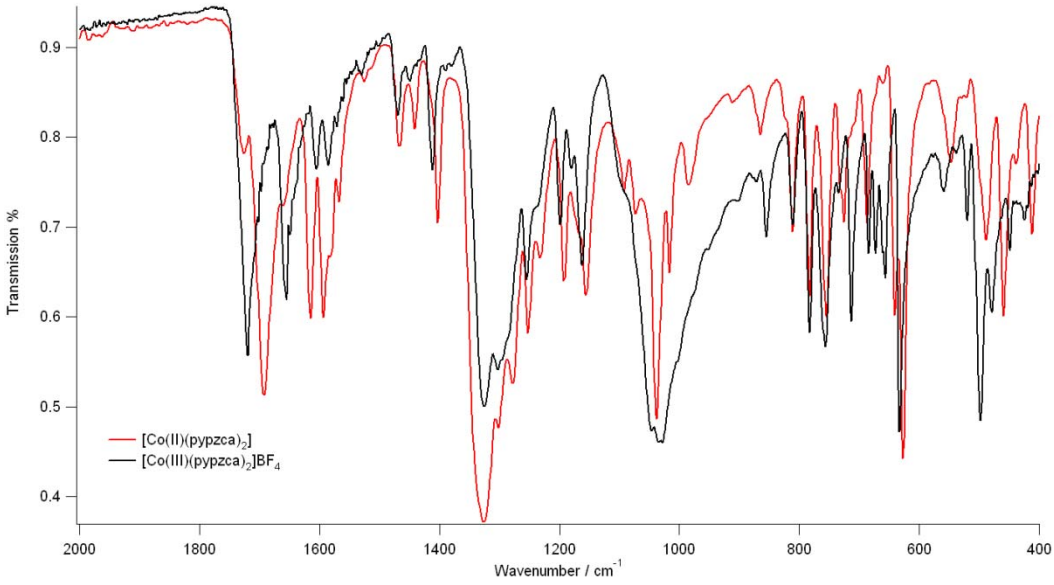

Figure S2. A comparison of the carbonyl stretching bands in $[Fe^{II}(pypzca)_2]$ and $[Fe^{III}(pypzca)_2]ClO_4$.

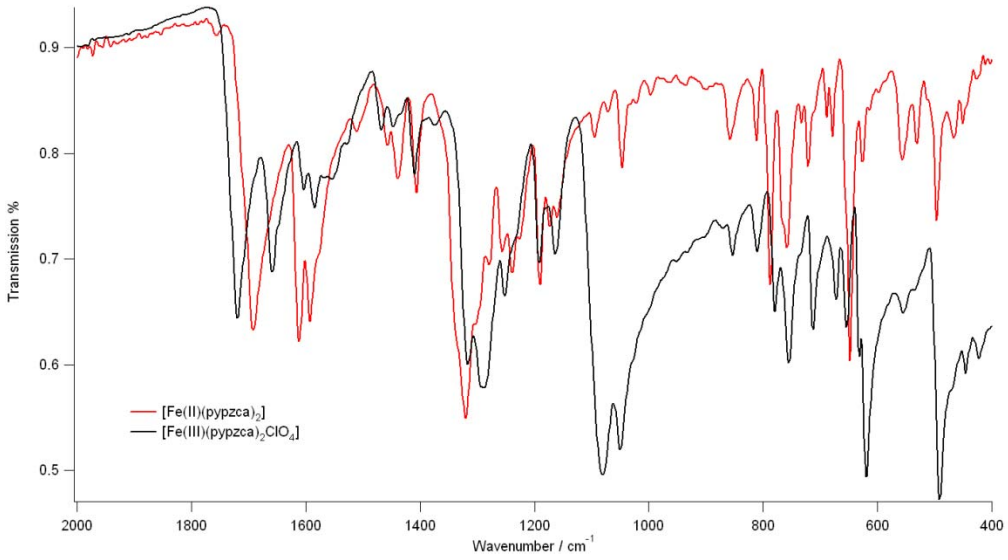

Crystal Data

Figure S3. The structure of ([Co^{II}(pypzca)$_2$]). Note that hydrogen atoms have been omitted for clarity.

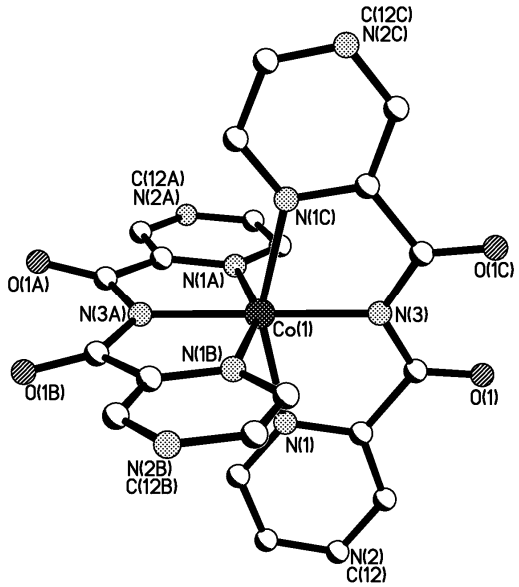

Figure S4. The crystal structure of one of the two crystallographically independent cations in the structure of ([Co^{III}(pypzca)$_2$]BF_4)$_2$. Note that the Co^{III} centre pulls the ligand tightly around it, facilitating orthogonality of the secondary assembly instructions. Note that hydrogen atoms and anions have been omitted for clarity.

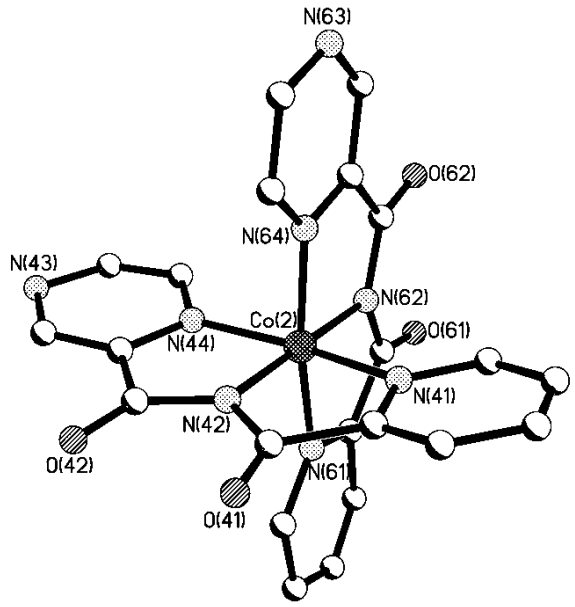

Figure S5. The packing of $[Cu^{II}(pypzca)(H_2O)_2]BF_4 \cdot H_2O$, illustrating the extensive hydrogen bonding network (O3 ⋯ O21 2.591; O21 ⋯ O4 2.789 Å).

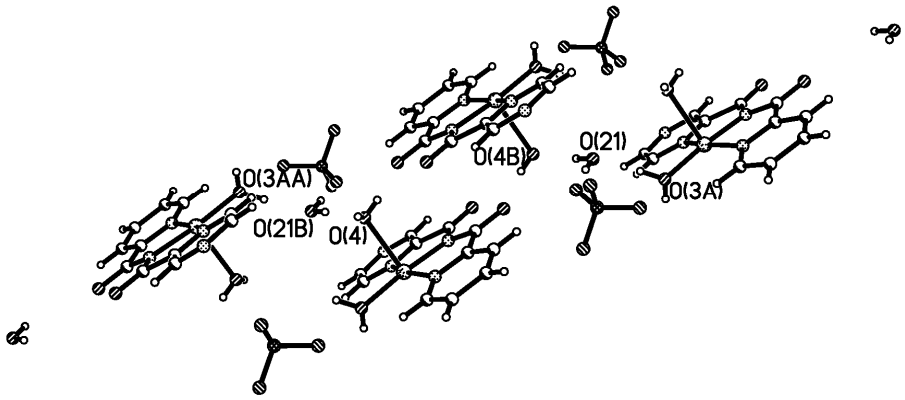

Table S1. Crystal structure determination details for the complexes $[Co^{III}(pypzca)_2]BF_4$, $[Co^{II}(pypzca)_2]$, $[Cu^{II}(pypzca)_2]$.

	$[Co^{III}L_2]BF_4$	**$[Cu^{II}L_2]$**	**$[Co^{II}L_2]$**
Empirical formula	$C_{22}H_{14}N_8O_4CoBF_4$	$C_{22}H_{15.5}N_8O_{4.75}Cu$	$C_{22}H_{14}N_8O_4Co$
M_r	600.15	531.46	513.34
Crystal system	Monoclinic	Monoclinic	Tetragonal
Space group	P2(1)/n	P2(1)/n	I4(1)/a
a [Å]	22.953(7)	9.3128(4)	8.6658(7)
b [Å]	8.540(3)	8.5744(3)	8.6658(7)
c [Å]	23.055(7)	28.3561(13)	27.721(2)
α [°]	90	90	90
β [°]	103.000(9)	97.046(2)	90
γ [°]	93	90	90
V [Å^3]	4403(2)	2247.2(2)	2081.7(1)
Z	8	4	4
T [K]	93(2)	90(2)	90(2)
$\rho_{calcd.}$ [gcm^{-3}]	1.811	1.571	1.638
μ [mm^{-1}]	0.867	1.024	0.88
F(000)	2416	1082	1044
Crystal size [mm]	0.20 x 0.20 x 0.02	0.30 x 0.22 x 0.10	0.3 x 0.2 x 0.1
Θ range for data collection [°]	1.13 to 13.26	2.78 to 26.37	2.46 to 26.40
Reflections collected	49902	38121	17823
Independent reflections	6313	4588	1074
R(int)	0.1746	0.0510	0.0399
Max. and min. transmission	1.000 and 0.6403	0.9045 and 0.7487	0.9175 and 0.8647
Data/ restraints/ parameters	6313 / 96 / 758	4588 / 0 / 329	1074 / 0 / 77
Goof (F^2)	1.069	1.067	1.113
R_1 [$I > 2\sigma(I)$]	0.1346	0.0463	0.606
wR_2 [all data]	0.3730	0.1477	0.1747

Table S2. Crystal structure determination details for the complexes $[Mn^{II}(pypzca)Cl_2]HN(CH_2CH_3)$ and $[Cu^{II}(pypzca)(H_2O)_2]BF_4.H_2O$.

	$[Mn^{II}(L)Cl_2]HNEt_3$	**$[Cu^{II}L(H_2O)_2]BF_4.H_2O$**
Empirical formula	$C_{17}H_{23}N_5O_2Cl_2Mn$	$C_{11}H_{13}N_4O_5BF_4Cu$
M_r	455.24	431.60
Crystal system	Monoclinic	Triclinic
Space group	P2(1)/c	P-1
a [Å]	7.9477(8)	8.1077(5)
b [Å]	18.030(2)	9.3487(6)
c [Å]	14.8985(18)	11.2246(7)
α [°]	90	92.472(4)
β [°]	99.695(6)	92.302(3)
γ [°]	90	110.049(3)
V [Å^3]	2104.5(4)	797.11(9)
Z	4	2
T [K]	90(2)	90(2)
$\rho_{calcd.}$ [gcm^{-3}]	1.437	1.798
μ [mm^{-1}]	0.903	1.447
F(000)	940	434
Crystal size [mm]	0.20 x 0.06 x 0.04	0.10 x 0.08 x 0.03
Θ range for data collection [°]	3.00 to 24.71	2.88 to 26.42
Reflections collected	35200	16738
Independent reflections	3586	3258
R(int)	0.0934	0.0485
Max. and min. transmission	0.9648 and 0.8401	0.7454 and 0.6761
Data/ restraints/ parameters	3586 / 45 / 274	3258 / 0 / 253
Goof (F^2)	1.278	1.065
R_1 [I > 2σ(I)]	0.0972	0.0382
wR_2 [all data]	0.2040	0.0833

Magnetic Data

Figure S6. The plot of magnetic moment vs. temperature for $[Fe^{III}(pypzca)_2]ClO_4$.

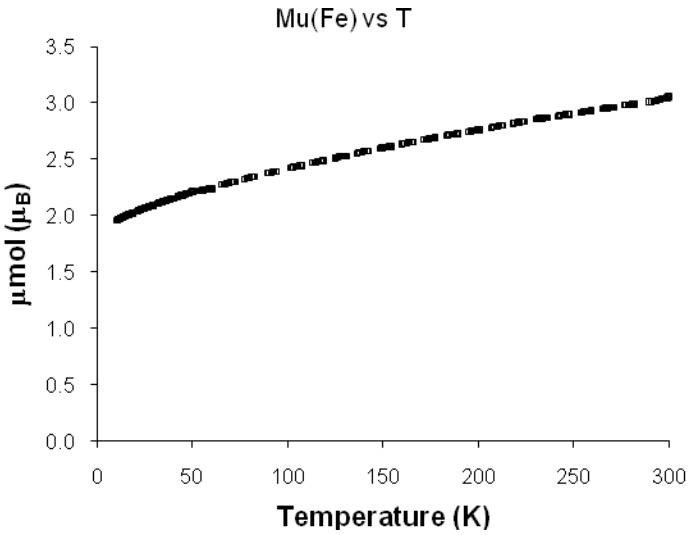

Figure S7. The plot of magnetic moment vs. temperature for $[Co^{II}(pypzca)_2]$.

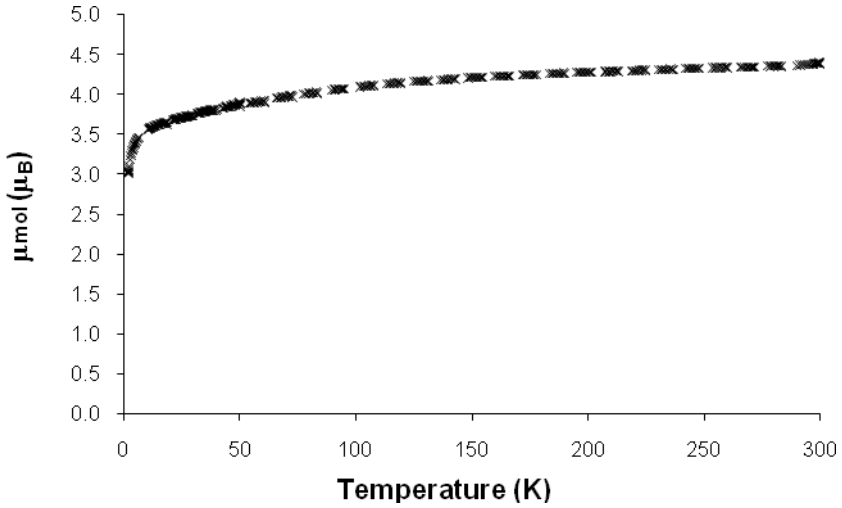

Figure S8. The plot of χT vs temperature for $[Co^{II}(pypzca)_2]$.

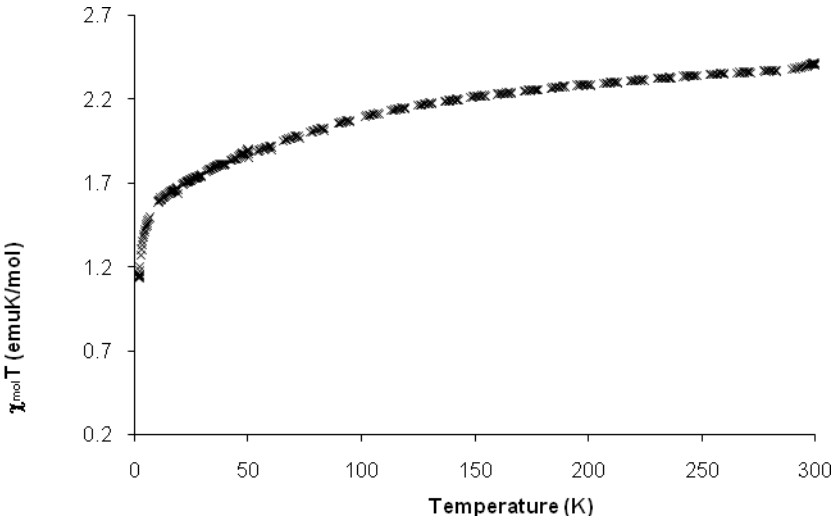

Figure S9. The plot of magnetic moment vs. temperature for $[Mn^{II}(pypzca)Cl_2]HNEt_3$.

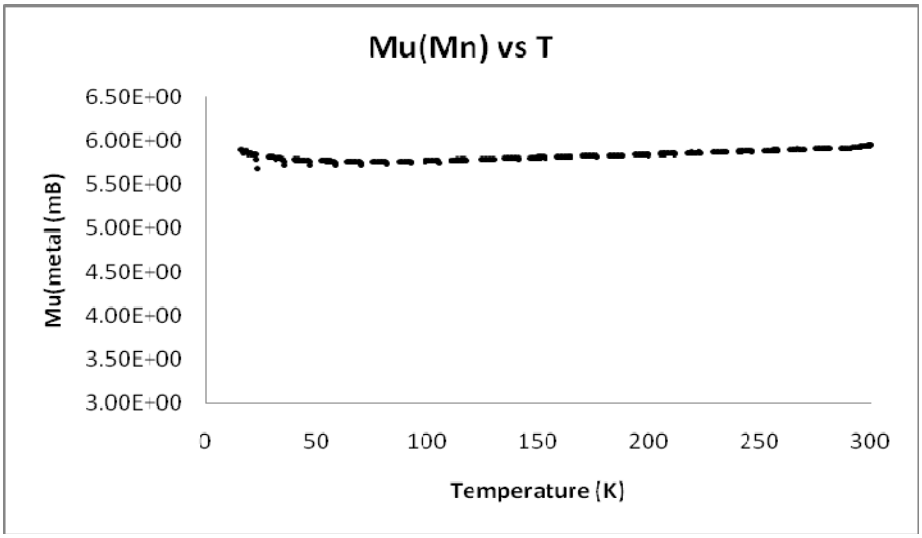

Cyclic Voltammetry Data

Experimental details of cyclic voltammetry studies can be found in the full paper.

Figure S10. Full cyclic voltammetry of $[Co^{III}(pypzca)_2]BF_4$. Scan rate 50 mVs^{-1}, ref 0.01 M $AgNO_3$/Ag.

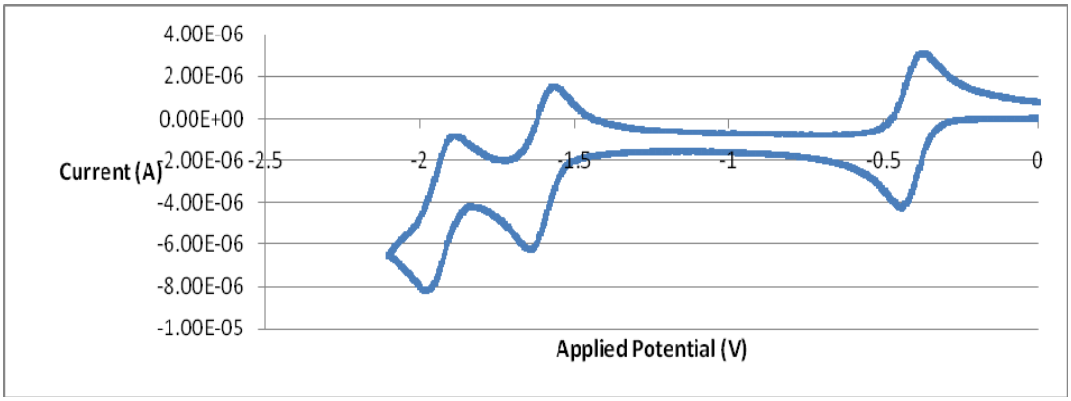

Scan Rate Studies of $[M(pypzca)_2]$ Metal Based Processes

Figure S11. Scan rate study of $[Ni^{II}(pypzca)_2]$.Ref 0.01 M $AgNO_3$/Ag.

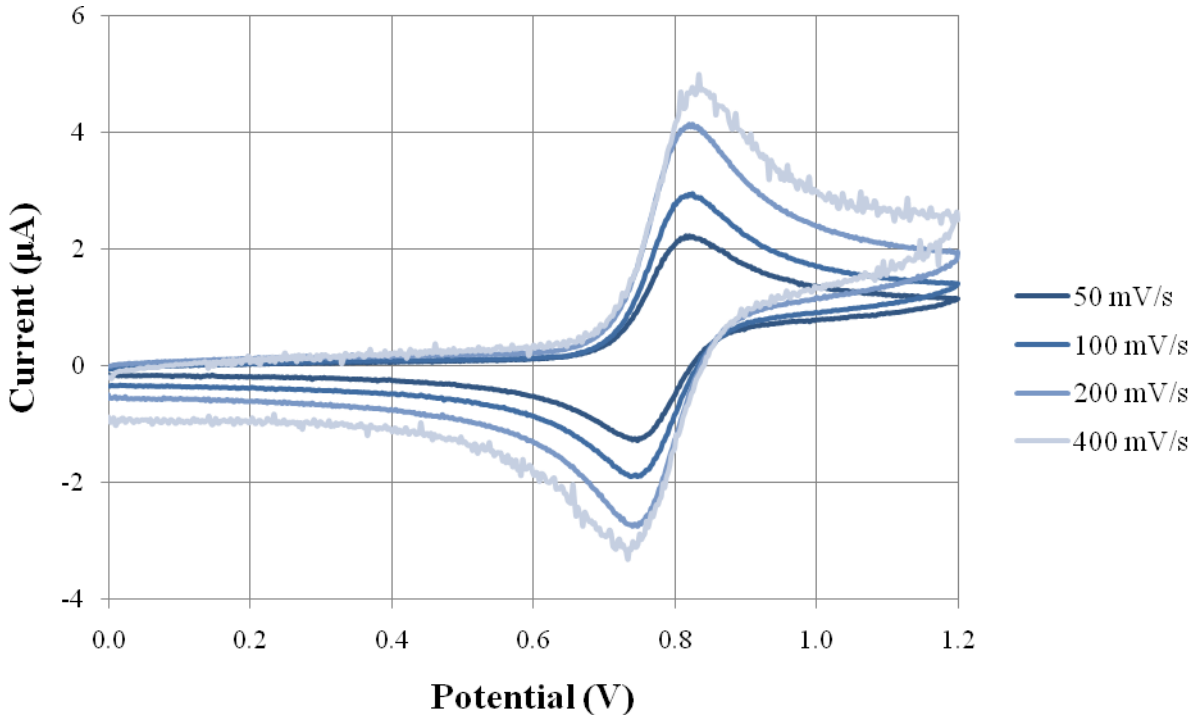

Figure S12. Scan rate study of $[Co^{III}(pypzca)_2]BF_4$.Ref 0.01 M $AgNO_3$/Ag.

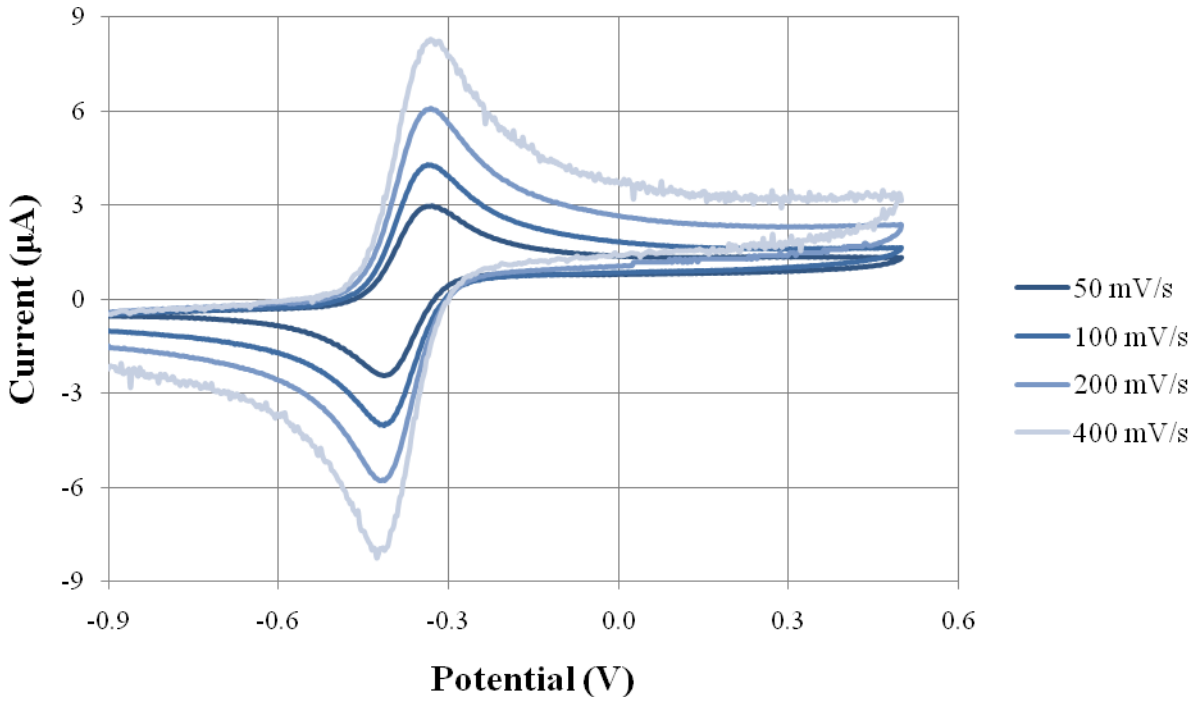

Figure S13. Scan rate study of $[Fe^{III}(pypzca)_2]ClO_4$.Ref 0.01 M $AgNO_3$/Ag.

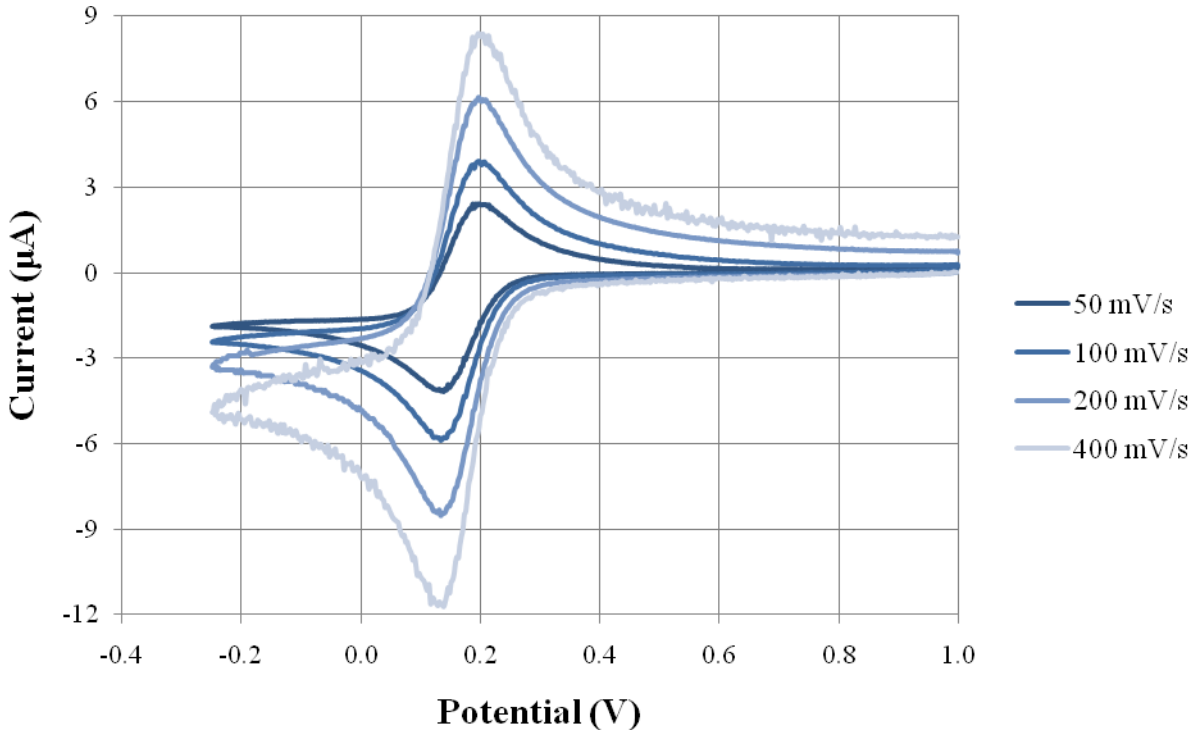

Figure S14. Full cyclic voltammetry of a suspension of $[Zn^{II}(pypzca)_2]$. Scan rate 200 mVs^{-1}, ref 0.01 M $AgNO_3$/Ag.

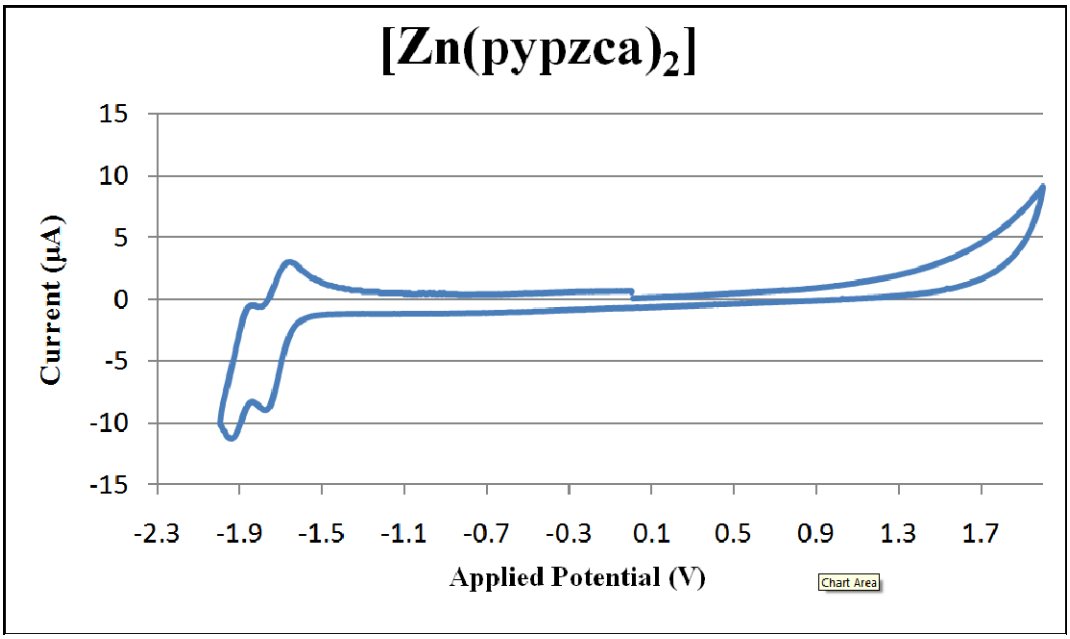

Cyclic Voltammetry of $[M^{II}(pypzca)_2]$; M = Co, Fe

Figure S15. Cyclic voltammetry of a suspension of $[Co^{II}(pypzca)_2]$ showing the metal based process. Scan rate 200 mVs^{-1}, ref 0.01 M $AgNO_3$/Ag.

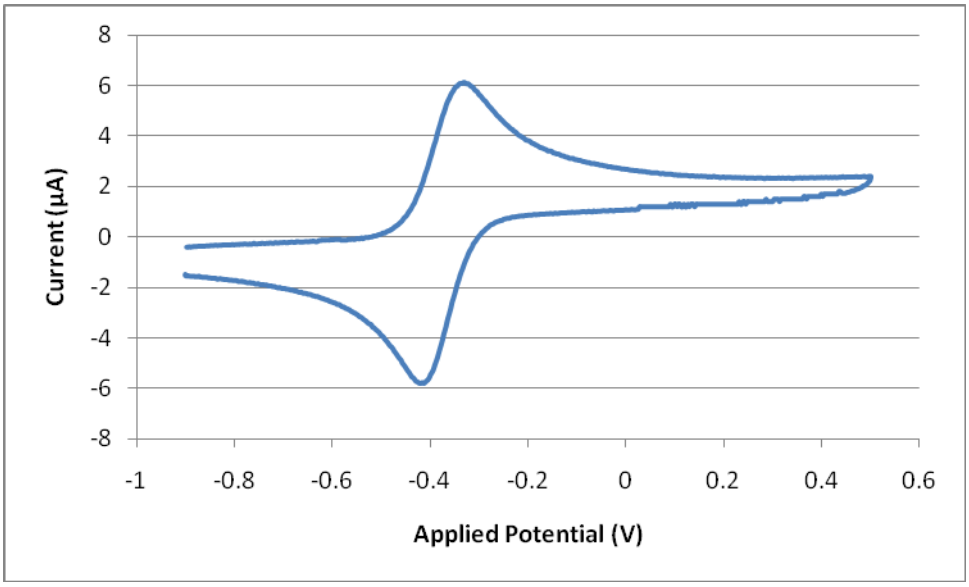

Figure S16. Cyclic voltammetry of a suspension of $[Fe^{II}(pypzca)_2]$ showing the metal based process. Scan rate 50 mVs^{-1}, ref 0.01 M $AgNO_3$/Ag.

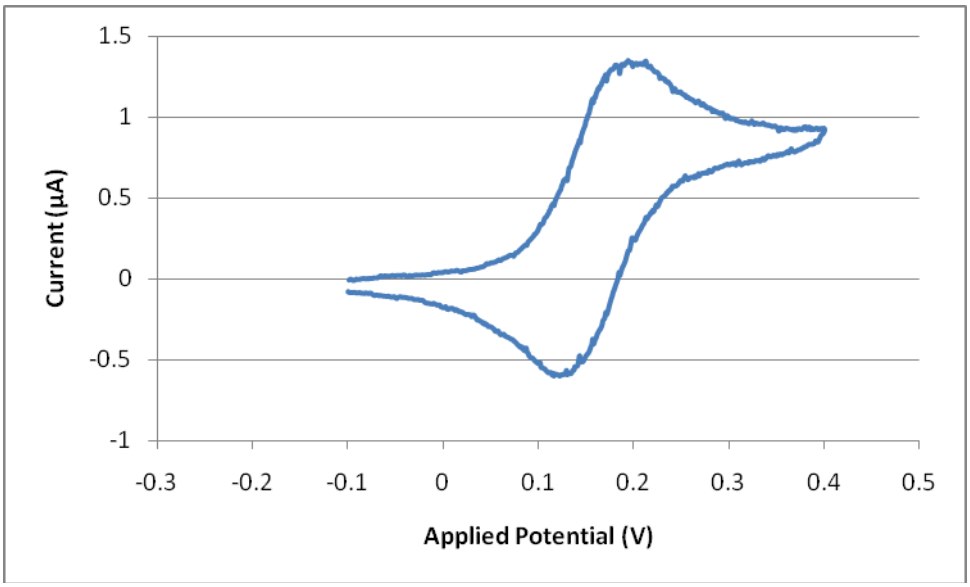

Figure S17. Cyclic voltammetry of a suspension of $[Co^{II}(pypzca)_2]$ showing the ligand based process. Scan rate 200 mVs^{-1}, ref 0.01 M $AgNO_3/Ag$.

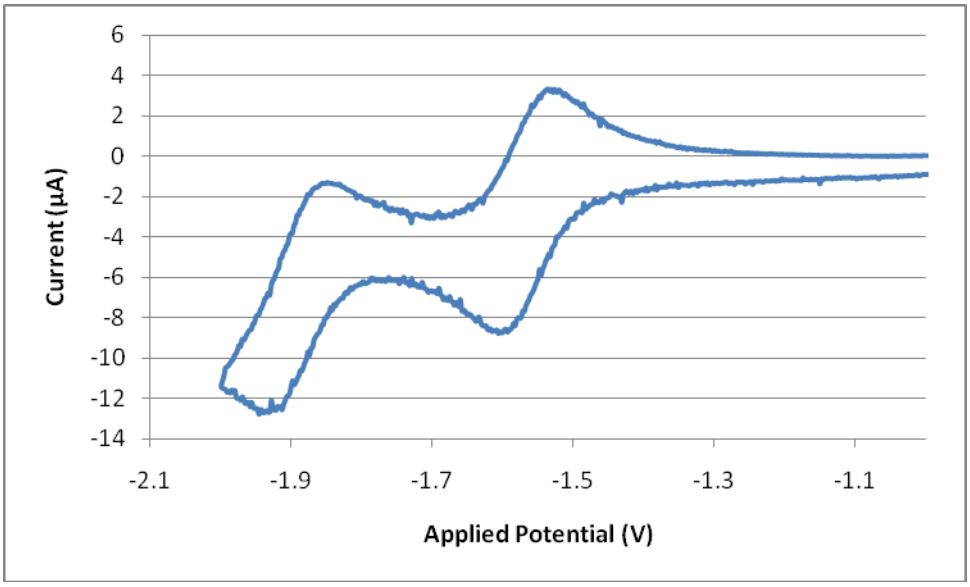

Figure S18. Cyclic voltammetry of a suspension of $[Fe^{II}(pypzca)_2]$ showing the ligand based processes. Scan rate 50 mVs^{-1}, ref 0.01 M $AgNO_3/Ag$.

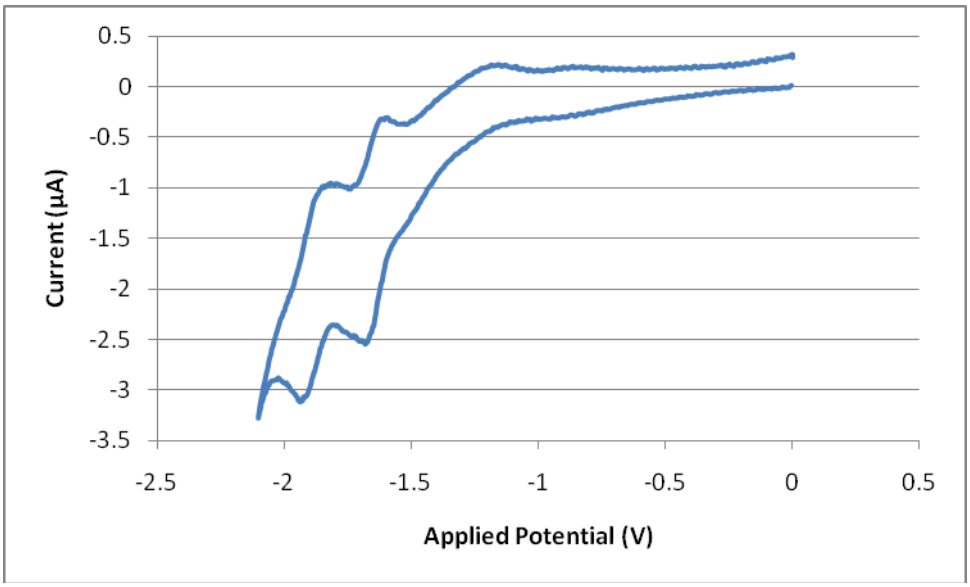

Scan Rate Studies of [M(pypzca)$_2$] Ligand Based Processes

Figure S19. Scan rate study of [Zn^{II}(pypzca)$_2$].Ref 0.01 M $AgNO_3$/Ag.

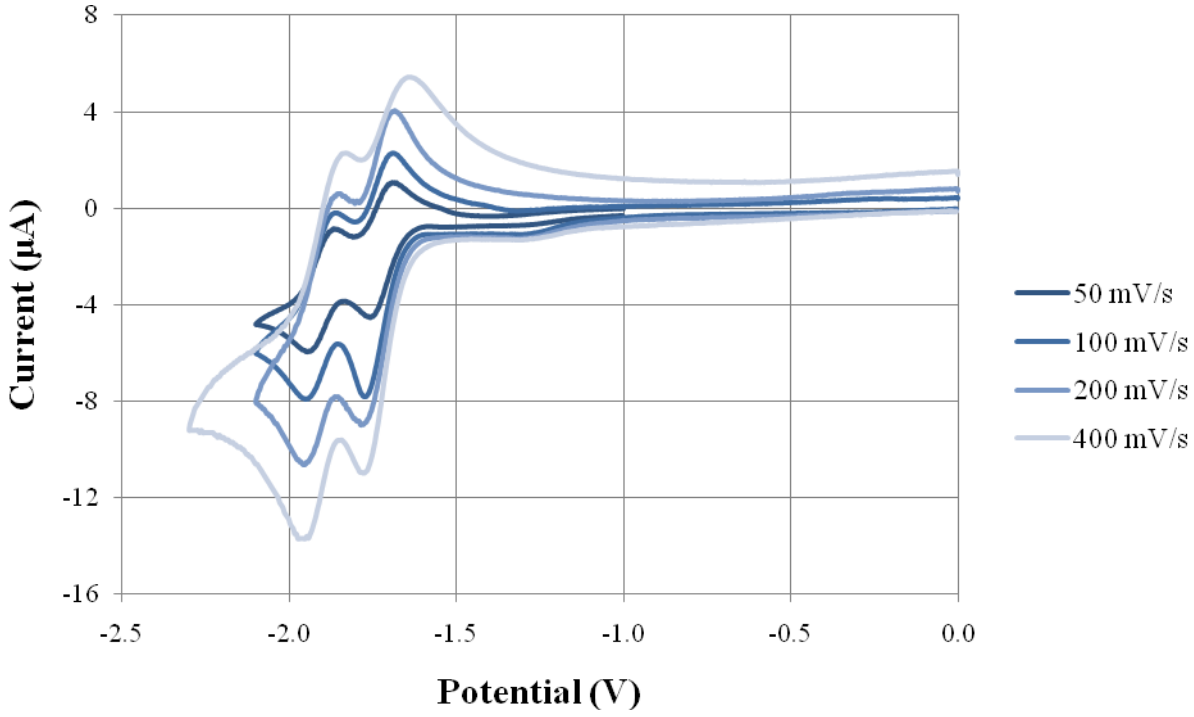

Figure S20. Scan rate study of [Ni^{II}(pypzca)$_2$].Ref 0.01 M $AgNO_3$/Ag.

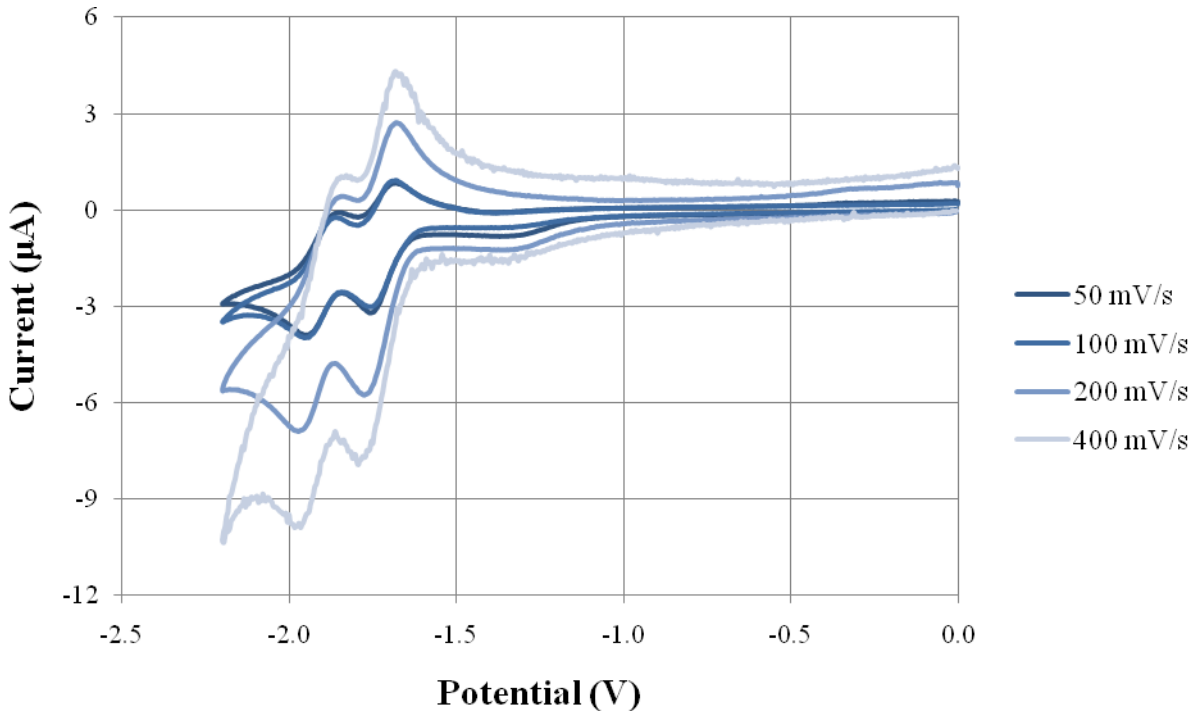

Figure S21. Scan rate study of $[Co^{III}(pypzca)_2]BF_4$.Ref 0.01 M $AgNO_3$/Ag.

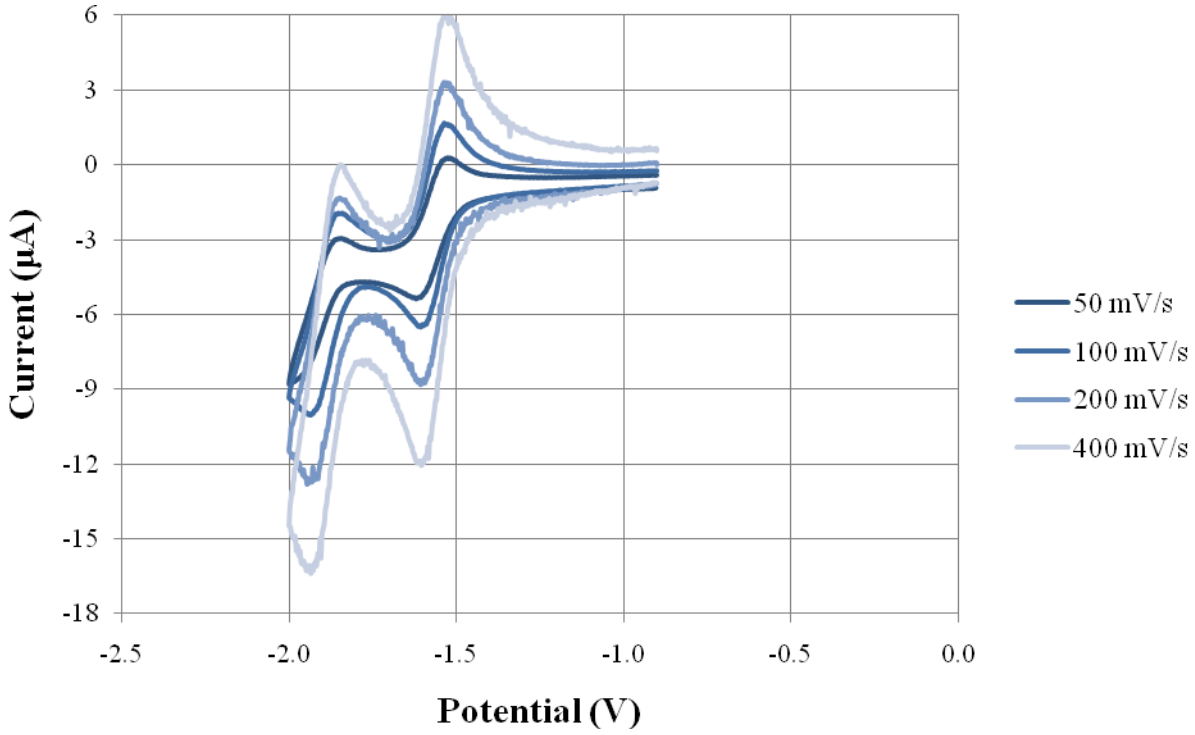

Figure S22. Scan rate study of $[Fe^{III}(pypzca)_2]ClO_4$.Ref 0.01 M $AgNO_3$/Ag.

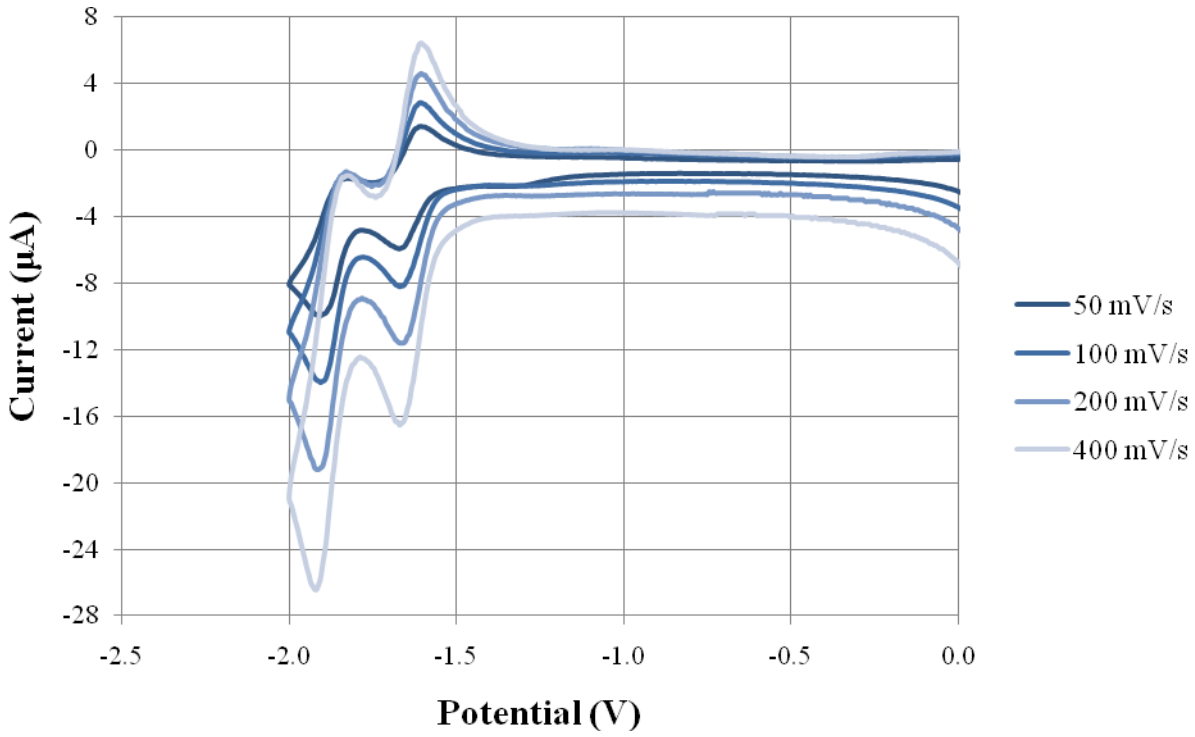

Cyclic Voltammetry of $[Cu^{II}(pypzca_2]$

Figure S23. Full scan of a suspension of $[Cu(pypzca)_2]$ starting at zero and going toward positive potentials. Scan rate 200 mVs^{-1}, ref 0.01 M $AgNO_3/Ag$.

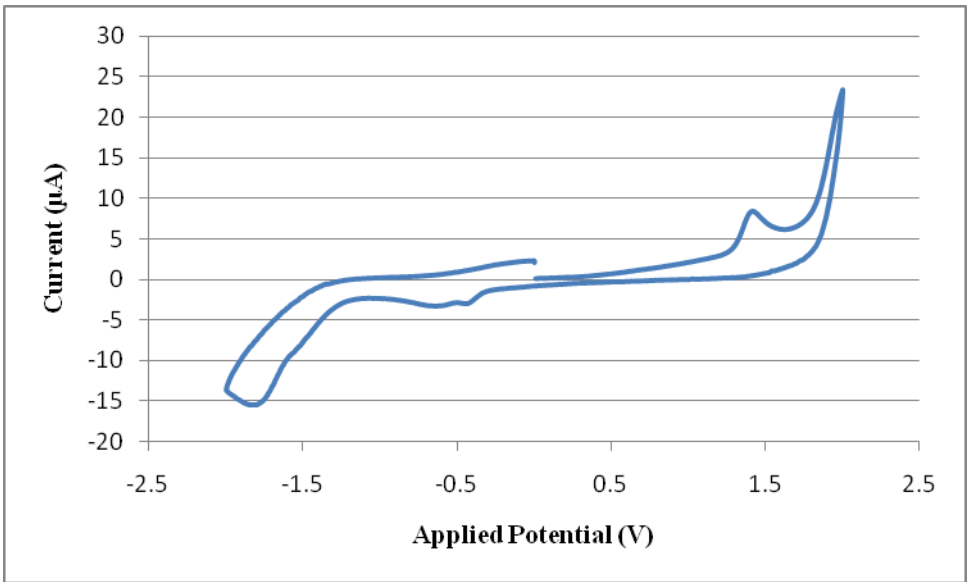

Figure S24. Full scan of a suspension of $[Cu(pypzca)_2]$ starting at zero and going toward negative potentials. Scan rate 200 mVs^{-1}, ref 0.01 M $AgNO_3/Ag$.

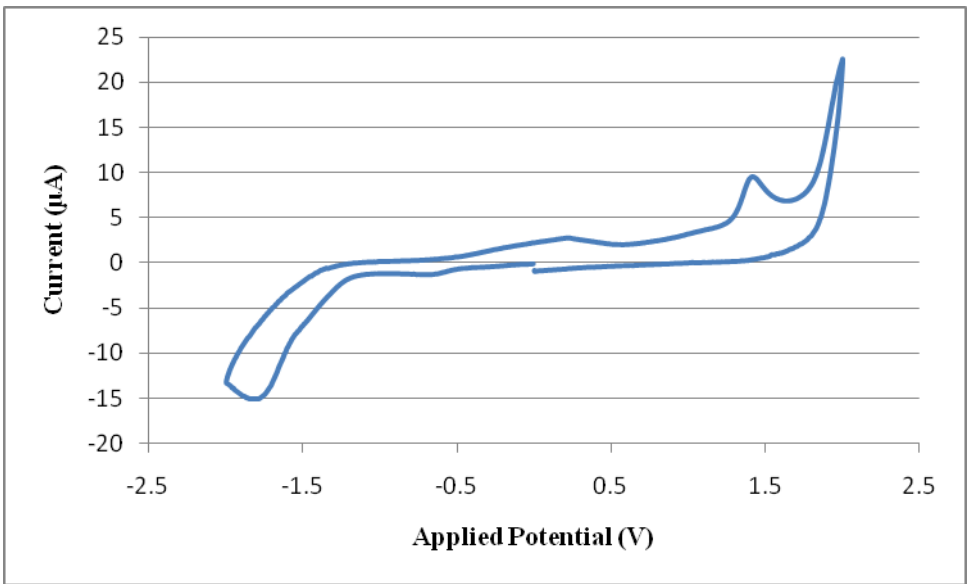

Cyclic Voltammetry of $[Cu^{II}(pypzca)(H_2O)_2]BF_4.H_2O$

Figure S25. Full scan of $[Cu^{II}(pypzca)(H_2O)_2]BF_4.H_2O$ starting at zero and going toward positive potentials. Scan rate 100 mVs^{-1}, ref 0.01 M $AgNO_3$/Ag.

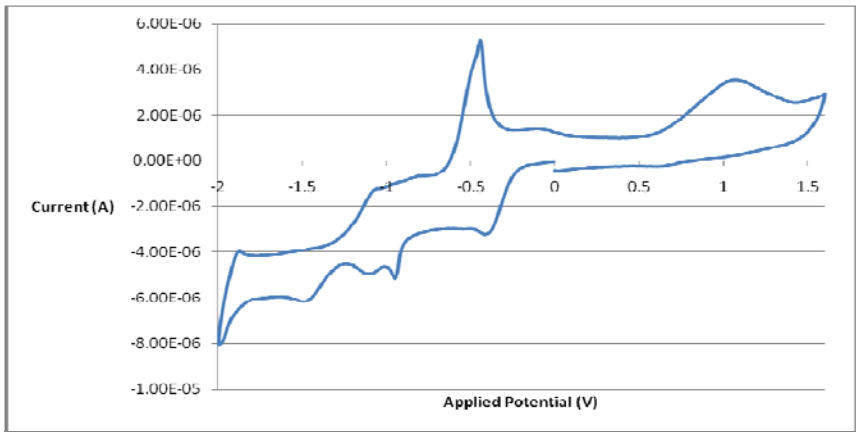

Figure S26. Full scan of $[Cu^{II}(pypzca)(H_2O)_2]BF_4.H_2O$ starting at zero and going toward negative potentials. Scan rate 100 mVs^{-1}, ref 0.01 M $AgNO_3$/Ag.

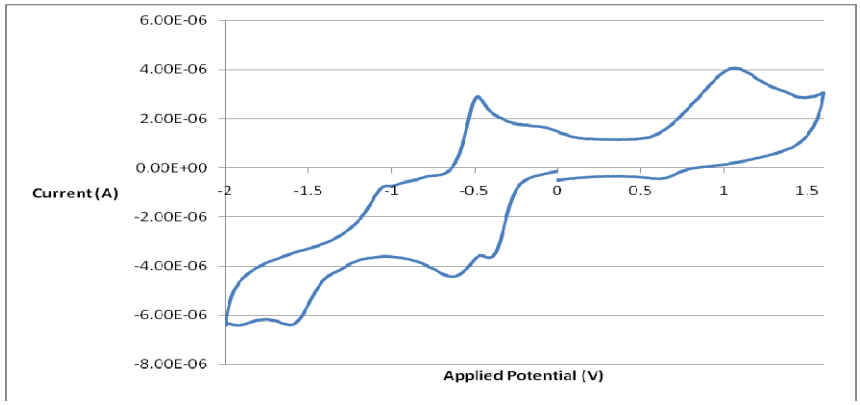

Figure S27. Scan of $[Cu^{II}(pypzca)(H_2O)_2]BF_4.H_2O$ between 0 and -1.7 V. Scan rate 100 mVs^{-1}, ref 0.01 M $AgNO_3$/Ag.

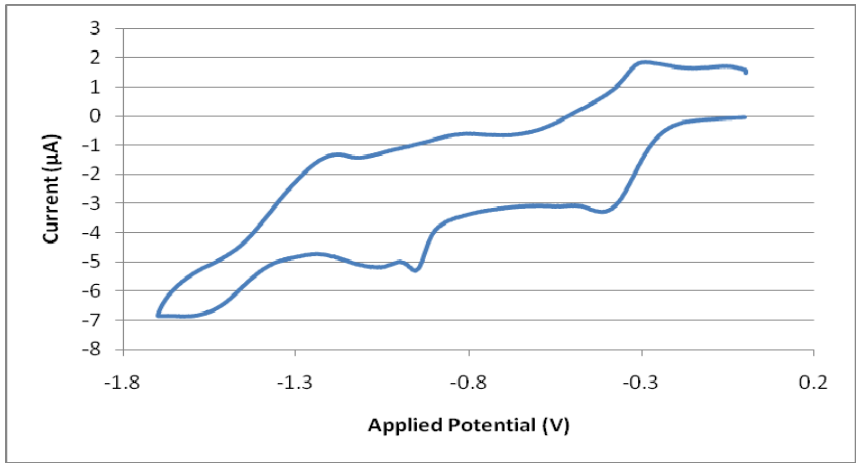

Cyclic Voltammetry of $[Mn^{II}LCl_2]HN(CH_2CH_3)_3$

Figure S28. Scan rate study of a 0.999 mmol L^{-1} suspension of $[Mn^{II}(pypzca)Cl_2]HNEt_3$.Ref 0.01 M $AgNO_3$/Ag.

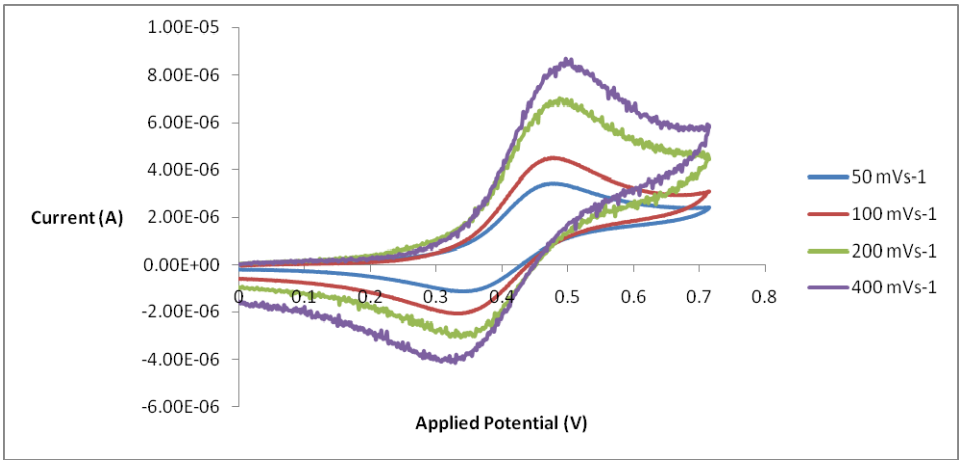

Figure S29. Scan rate study of a 10 mL acetonitrile solution of $[Mn^{II}(pypzca)Cl_2]HN(CH_2CH_3)_3$ (1.14 mmol L^{-1}) after bulk electrolysis to 0.6 V.

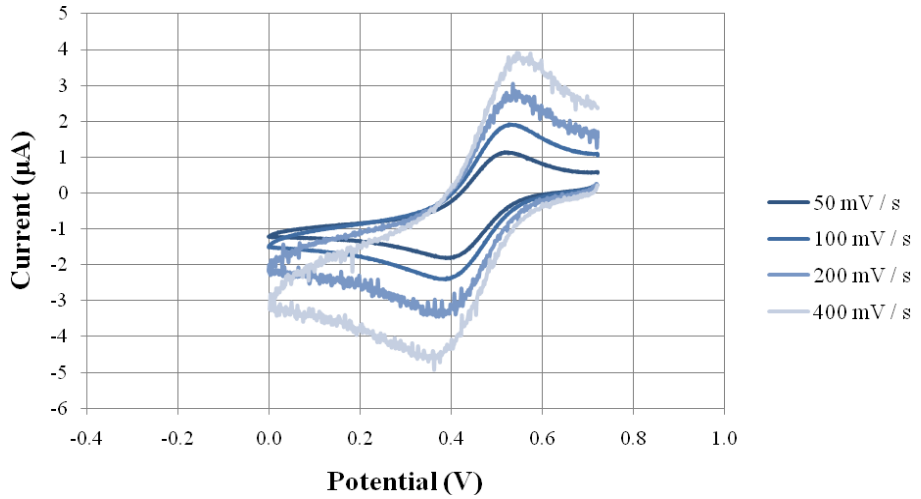

Figure S30. Full scan of a 1.5 mmol suspension of $[Mn^{II}(pypzca)Cl_2]HNEt_3$ starting at zero and going toward positive (left) or negative (right) potentials. Scan rate 200 mVs^{-1}, ref 0.01 M $AgNO_3$/Ag.

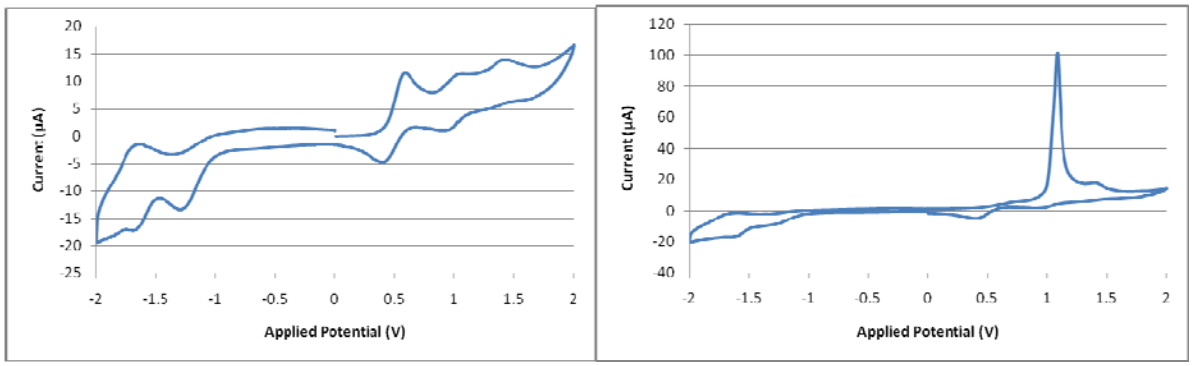

Figure S31. Full scan of a 1.5 mmol solution of $[Mn^{II}(pypzca)Cl_2]HNEt_3$ after bulk electrolysis to 0.6 V starting at zero and going toward positive (left) or negative (right) potentials. Scan rate 200 mVs^{-1}, ref 0.01 M $AgNO_3$/Ag.

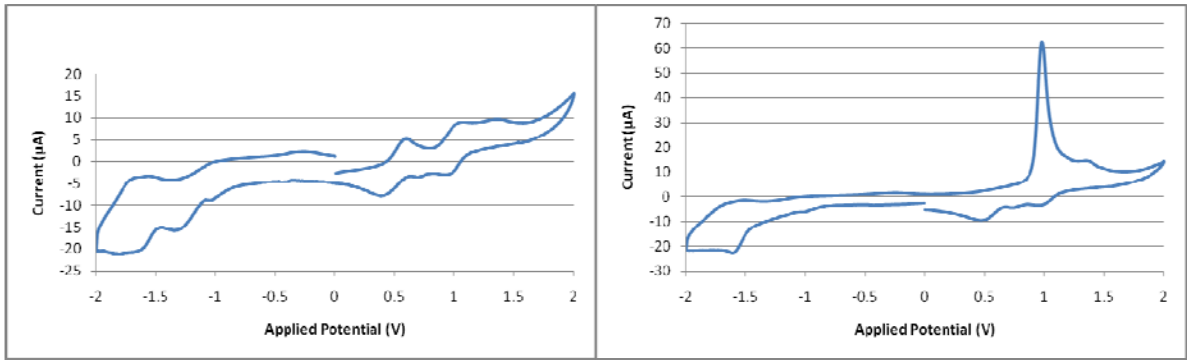

Figure S32. Full scan of a 1.5 mmol solution of $[Mn^{II}(pypzca)Cl_2]HNEt_3$ after bulk electrolysis to 0.6 V then 0 V starting at zero and going toward positive (left) or negative (right) potentials. Scan rate 200 mVs^{-1}, ref 0.01 M $AgNO_3$/Ag.

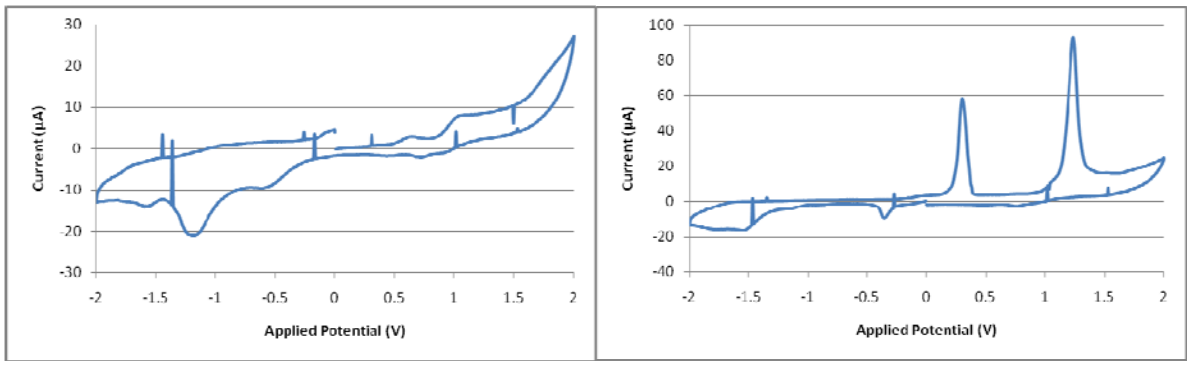

Bulk Electrolysis

Table S3. Bulk electrolysis results for $[M^{n}(pypzca)_2]^{n-2+}$ complexes.

Complex	Applied Potential	Charge Passed (% electron)	Colour Change
$[Zn^{II}(pypzca)_2]$	-1.75 V	160	Colourless to yellow
$[Ni^{II}(pypzca)_2]$	0.87 V	88	Light brown to green
$[Fe^{II}(pypzca)_2]$	0.30 V	97	Purple to light brown
$[Co^{II}(pypzca)_2]$	-0.20 V	71	Light orange to golden red
$[Fe^{III}(pypzca)_2]ClO_4$	0.63V	82	Yellow to purple
$[Co^{III}(pypzca)_2]BF_4$	-0.55 V	89	Golden red to light orange/yellow
$[Mn^{II}(pypzca)Cl_2]HNEt_3$	0.60 V	47, 52, 53*	Light green to light brown

*Was repeated to reproduce the unexpected result

Figure S33. Bulk electrolysis of a 10 mL acetonitrile solution of $[Mn^{II}(pypzca)Cl_2]HN(CH_2CH_3)_3$ (0.999 mmol L^{-1}) showing the decrease of current over time. Applied potential of 0 V.

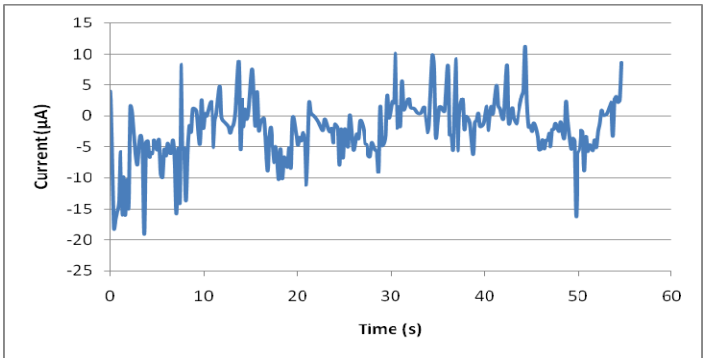

Figure S34. Bulk electrolysis of a 10 mL acetonitrile solution of $[Mn^{II}(pypzca)Cl_2]HN(CH_2CH_3)_3$ (0.999 mmol L^{-1}) showing the decrease of current over time. Applied potential of 0.6 V.

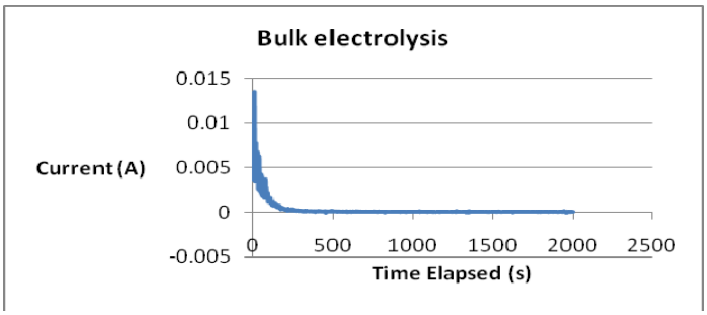

Figure S35. Bulk electrolysis of a 10 mL acetonitrile solution of $[Mn^{II}(pypzca)Cl_2]HN(CH_2CH_3)_3$ (0.999 mmol L^{-1}) showing the transfer of charge over time. Applied potential of 0.6 V. Charge passed at 2000 seconds: 0.52 Q.

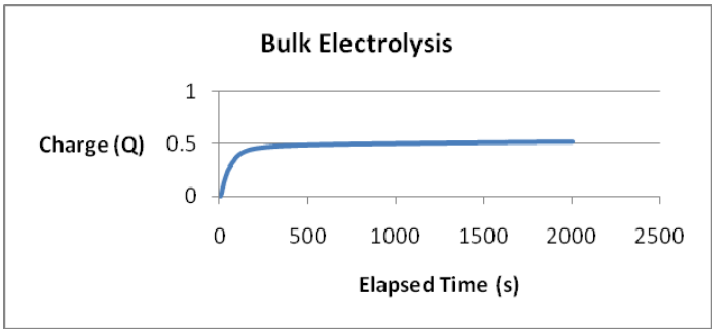

Figure S36. Bulk electrolysis at 0.576 V of a different 10 mL acetonitrile solution of $[Mn^{II}(pypzca)Cl_2]HN(CH_2CH_3)_3$ (1.14 mmol L^{-1}) showing the decrease of current over time:

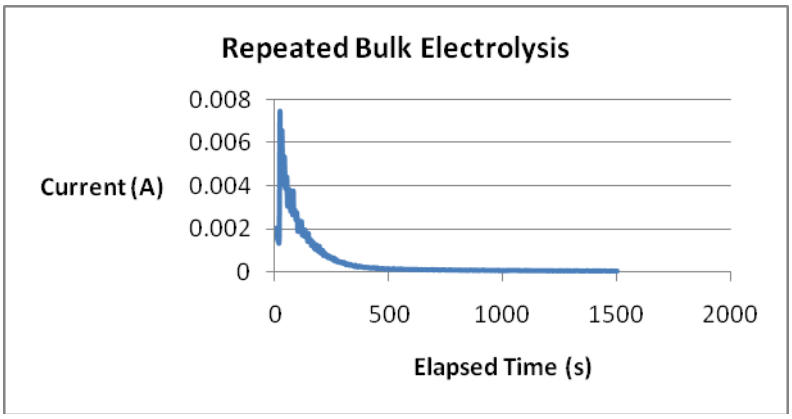

Figure S37. Bulk electrolysis of a different 10 mL acetonitrile solution of $[Mn^{II}(pypzca)Cl_2]HN(CH_2CH_3)_3$ (1.14 mmol L^{-1}) showing the transfer of charge over time. Applied potential of 0.576 V. Charge passed at 1500 seconds: 0.64 Q.

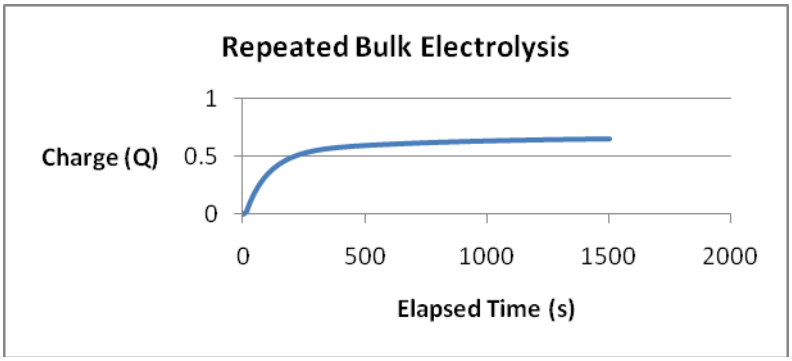

Figure S38. Bulk electrolysis at 0.6 V of a different 10 mL acetonitrile solution of $[Mn^{II}(pypzca)Cl_2]HN(CH_2CH_3)_3$ (1.70 mmol L^{-1}) showing the decrease of current over time.

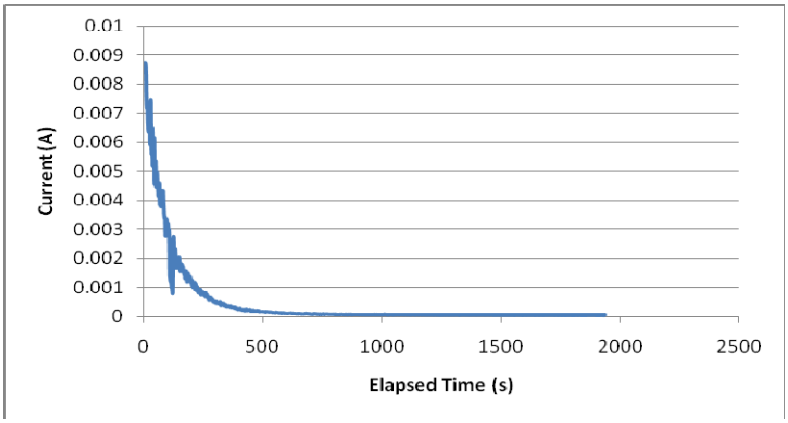

Figure S39. Bulk electrolysis of a third 10 mL acetonitrile solution of $[Mn^{II}(pypzca)Cl_2]HN(CH_2CH_3)_3$ (1.7 mmol L^{-1}) showing the transfer of charge over time. Applied potential of 0. 6 V. Charge passed at 1932 seconds, 895 Q; 0.53 electrons per molecule.

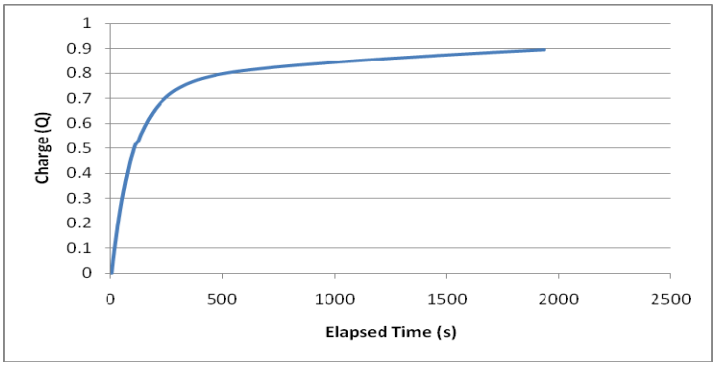

Figure S40. Bulk electrolysis to 0 V after bulk electrolysis to 0.6 V of a third 10 mL acetonitrile solution of $[Mn^{II}(pypzca)Cl_2]HN(CH_2CH_3)_3$ (1.7 mmol L^{-1}) showing the decrease of current over time:

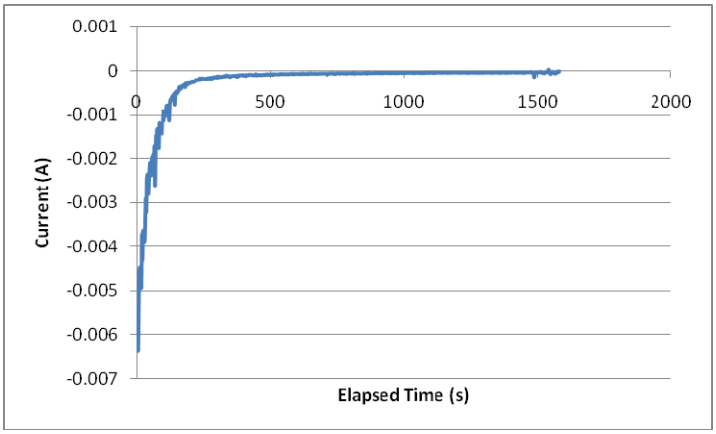

Figure S41. Bulk electrolysis to 0 V after bulk electrolysis to 0.6 V of a third 10 mL acetonitrile solution of $[Mn^{II}(pypzca)Cl_2]HN(CH_2CH_3)_3$ (1.70 mmol L^{-1}) showing the transfer of charge over time. Applied potential of 0. 6 V. Charge passed at 1534 seconds: 0.42 Q.

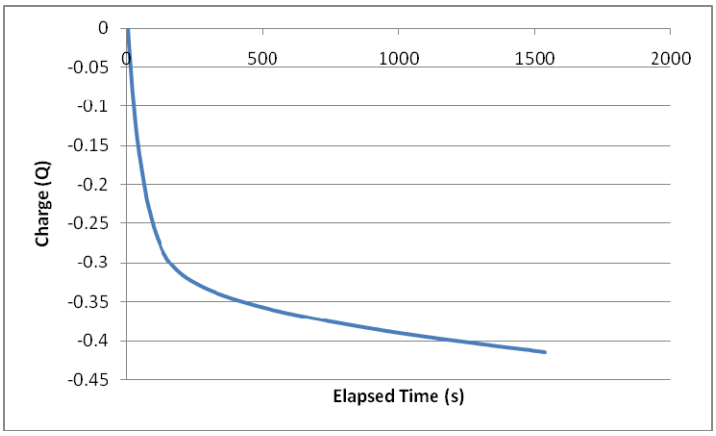

Figure S42. Bulk electrolysis to 0.6 V after bulk electrolysis 0 V after bulk electrolysis to 0.6 V of a third 10 mL acetonitrile solution of $[Mn^{II}(pypzca)Cl_2]HN(CH_2CH_3)_3$ (1.70 mmol L^{-1}) showing the decrease of current over time:

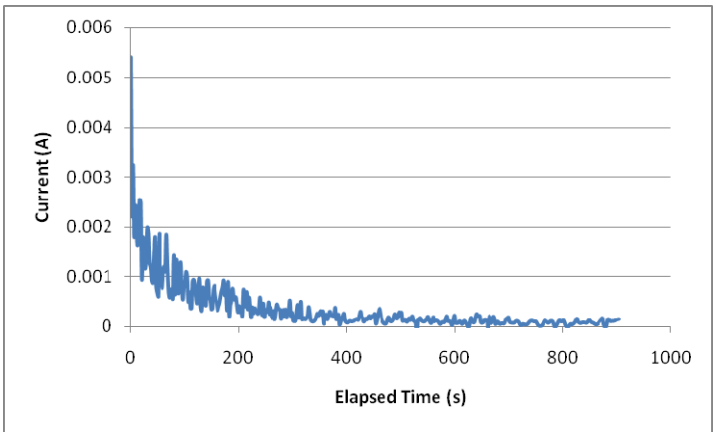

Figure S43. Bulk electrolysis to 0.6 V after bulk electrolysis 0 V after bulk electrolysis to 0.6 V of a third 10 mL acetonitrile solution of $[Mn^{II}(pypzca)Cl_2]HN(CH_2CH_3)_3$ (1.70 mmol L^{-1}) showing the transfer of charge over time. Applied potential of 0. 6 V. Charge passed at 899 seconds: 0.30 Q.